CALIFORNIA INSTITUTE OF TECHNOLOGY

EARTHQUAKE ENGINEERING RESEARCH LABORATORY

INTERPRETATION OF MILLIKAN LIBRARY'S VIBRATING MODES USING A MAGNETO COIL TO MEASURE PHASE SHIFTS

BY

MING HEI CHENG, THOMAS H. HEATON AND MONICA D. KOHLER

REPORT NO. EERL 2014-02

PASADENA, CALIFORNIA

DECEMBER 2014

Interpretation of Millikan Library's Vibrating Modes Using a Magneto Coil to Measure Phase Shifts

Ming Hei Cheng, Thomas H. Heaton, and Monica D. Kohler

Department of Mechanical and Civil Engineering, California Institute of Technology

Abstract

A new set of natural frequencies for the 9-story reinforced concrete Millikan Library building on the Caltech campus is computed using the observed phase shift between the driving force of a shaker installed on the building's roof and structural response at resonance. The phase of the shaker's output force was recorded by a magneto coil and magnet attached to the shaker's rotating mechanism, and the phase of the structural response was obtained from acceleration time series recorded by an accelerometer on the roof. These new results refute previous studies' identification of the 3rd EW and 2nd torsional modes which used spectral analysis of forced and free vibrations, but did not consider the phase shift. In addition, the newly identified 3rd EW mode shape is independent of the other EW mode shapes, unlike previous findings. This new interpretation is compatible with results from subspace system identification based on two sets of earthquake records.

Keywords: Millikan Library; natural frequency; phase shift; magneto coil; subspace system identification

1. Introduction

Phase shifts relate to the time lag between an input excitation and a vibrating mechanical system's response, and can be effective in identifying the natural frequencies of a dynamic system. Techniques using measured phase shifts have been adopted in various engineering applications such as the design of beam resonators in Microelectromechanical Systems (MEMS) (e.g. Piekarski et al., 2001; Scheible and Blick, 2004) and the design of Electromagnetic Suspension systems (EMS) in maglev trains (e.g. Wang et al., 2008; Zhou et al., 2011). These studies motivate the work presented here in which we use phase shift measurements between a driving force and the resulting structural response to identify the normal modes of the Millikan Library building on the Caltech campus.

Millikan Library (Fig. 1) is a reinforced concrete building with nine stories and one level of basement. It has a stiff core wall that encases the elevators and a stairwell. In addition, there are 30-cm thick shear walls on the east and west sides of the building which make the building very stiff in the NS direction (the first NS modal frequency is 1.7 Hz). EW vibrations are resisted by a

combination of the core wall and massive moment frames (the first EW frequency is 1.15 Hz). A Kinemetrics VG-1 shaker with counter-rotating weight baskets has been installed on the roof for the past 40 years and it has been used frequently for a variety of research and class projects. Since Millikan Library was constructed in 1966, its natural frequencies have been monitored. The NS, EW and torsional natural frequencies of the first two modes obtained from forced vibration tests, ambient vibration tests, and several earthquakes are well documented (e.g. Udwadia and Trifunac, 1974; Foutch and Jennings, 1978; Luco et al., 1987). Todorovska (2009a, b) estimated the 1st mode natural frequencies using the spectral peak of the transfer function between the roof response and the ground response for four earthquakes. Michel and Gueguen (2010) adopted a pseudo-Wigner-Ville method to address the variation of 1st mode natural frequencies during earthquakes. Bradford et al. (2004) and Clinton et al. (2006) estimated the higher mode natural frequencies through forced vibration experiments. The frequencies were identified based on the spectral peaks of roof displacement records.

The previously proposed 3rd EW mode for Millikan Library is problematic because the corresponding mode shape is not independent of the other EW modes. The 1st mode has no zero-crossings, the 2nd mode has one zero-crossing, but the 3rd mode also has only one zero-crossing. These previously proposed mode shapes are shown in Fig. 2. In this study, a new set of natural frequencies for the Millikan Library building is proposed using the observed phase shift between the driving force and the building's response at resonance, a parameter that was not considered in the previous studies. The results presented here show that the newly identified 3rd EW mode shape is independent of the other EW modes.

In this study, the phase shifts were measured by recording the voltage from a magneto coil and magnet that was attached to the shaker producing the forced vibrations. The results from the phase shift experiment can serve as an independent measure of natural frequencies. The new interpretation of natural frequencies presented here are compatible with the results from deterministic-stochastic subspace identification. Subspace system identification using both input and output data has been used extensively to extract modal parameters, including natural frequencies, damping ratios and mode shapes from civil engineering structures (e.g. Overschee, 1994; Ljung, 1999; Guyader and Mevel, 2003; Moaveni and Asgarieh, 2012).

2. Using phase shifts to identify modal frequencies

Measurements of the spectral amplitude of the roof motions of Millikan Library have been used to identify natural frequencies by other researchers. While this methodology is clearly effective for identifying the 1st NS, EW, and torsional modes of the building (Li et al., 2002; Arakawa and Yamamoto, 2004; Bradford et al., 2004), identifying the higher modes from spectral peaks is ambiguous. Therefore, we use a phase shift experiment to assist in the identification of higher modes. Assuming Rayleigh damping, the time-dependent response of a single building mode is

identical to that of a single-degree-of-freedom damped linear oscillator (Taylor, 2005; Chopra, 2007). Consider a single-degree-of-freedom damped oscillator that is driven by a sinusoidal driving force. The phase shift δ that describes the lag (in degrees) of the oscillator's motion behind the driving force is

$$\delta = arctan(\frac{2\beta\omega}{\omega_0^2-\omega^2}) \quad (1)$$

where β is the damping constant, ω_0 is the natural frequency of the system, and ω is the driving frequency.

When $\omega \ll \omega_0$, the oscillator's response is in phase with the driving force and δ is zero or negligible. As ω increases, δ also increases. When $\omega = \omega_0$, the argument of the arctan function in Eq. 1 is infinity and the oscillator lags 90^o behind the driving force; if the forcing function is sinusoidal, then the response is cosinusoidal. When $\omega > \omega_0$, the argument of the arctan function is negative and becomes zero as ω increases until the oscillator becomes 180^o out of phase with the driving force. As the damping of the system is decreased, the rate of change of the phase becomes larger at the resonant frequency. However, at the resonant frequency, the phase lag is always 90^o (Fig. 3). For a building with multiple independent vibrating modes, the phase lag will always be 90^o at each of its natural frequencies. Even without the assistance of mode shapes, vibrating modes of a building can be easily identified by the observed phase shift between the driving force and the structural response.

Forced vibration experiments have been performed for decades using the shaker installed on the roof of Millikan Library. However, no previously published work has compared the phase lag between the shaker and the building's acceleration response. To measure the shaker's cyclic motion, in light of the problem with the orthogonality of mode shapes for previously proposed modes, we constructed a simple magneto device to record shaker phase data (Fig. 4). The magneto coil was affixed to the cage of the shaker and a tiny magnet was attached to the bucket of the shaker. A sharp impulse voltage was generated when the magnet passed under the magneto device. This occurred every time the two counter-rotating buckets overlapped, generating the maximum input force from the shaker.

For a single-degree-of-freedom system, the phase difference between the harmonic input driving force and the system response increases from 0^o to 180^o as the driving frequency increases from just below to just above the natural frequency. It is not as easy to identify such phase shifts from 0^o to 180^o for the higher modes of a multi-degree-of-freedom system, especially when there are several modes with similar frequencies. Since we are really only interested in identifying modal frequencies, we are only interested in finding cases when the building motion is 90^o out of phase with the shaker force.

A shaker frequency sweep experiment was conducted on July 31, 2011 for Millikan Library. No lead weights (i.e., the buckets that hold the lead weights were empty) were used in the shaker during the experiment. The driving frequency was increased from 0.9 Hz to 9.7 Hz (the maximum allowable), incrementally by 0.05 Hz. The magneto device time series voltage data was recorded on a 24-bit datalogger which uses GPS-based time synchronization via an external antenna. The recorded data was then compared to the building roof response which was extracted from 24-bit accelerometer data (station "MIK" provided by the Southern California Earthquake Data Center archive).

The time history plots from the experiment are shown in Figs. 5-10. The acceleration records are filtered using a second-order Butterworth bandpass filter with a half-width of 0.15 Hz centered on the excitation frequency. The vertical dotted lines indicate the time at which the shaker generates the maximum force, i.e. the peaks of the sinusoidal output. At resonance, the sharp voltage spike occurs when the building response has zero amplitude; i.e. the building and shaker are 90^o out of phase. Note that the figures are plotted with different time scales because building response takes less time to complete one cycle at higher frequencies than at lower frequencies.

Fig. 5 shows the recorded building acceleration from the roof (station "MIK") when the shaker is driven at 1.15 Hz, the frequency of the 1^{st} EW mode. Fig. 5(a) and 5(c) display the EW and NS acceleration time series respectively, recorded during EW forcing by the shaker at maximum excitation of that mode. Fig. 5(b) and 5(d) similarly display the EW and NS acceleration time series for NS forcing by the shaker, which is nearly orthogonal to the EW mode. As expected, driving the shaker at the building's 1^{st} EW mode frequency in the EW direction results in a clear 90^o phase shift between the magneto output and the building motion. All other phase shifts are zero, except for the NS building response during the EW forcing by the shaker. This illustrates that the building does not oscillate in a purely EW direction; it exhibits a minor component of NS motion.

Similarly, the data for the 1^{st} NS mode at 1.7 Hz (Fig. 6) shows that the building does not oscillate in pure NS motion, but also exhibits a minor component of EW motion. Fig. 7 shows the 1^{st} torsional mode that occurs at 2.4 Hz. The shaker is located approximately 6.1 m south of the center of mass of the building, as shown in Fig. 1. Due to the off-center location of the shaker, it is more likely to trigger the torsional response of the building during the EW forcing than during NS forcing. Since the driving force is not perfectly aligned in any one direction, an eccentric force is generated in the EW direction when the shaker is operated in the NS direction, and vice versa. Both the NS and EW building responses during the EW excitation of the shaker at the 1^{st} torsional modal frequency show a clear 90^o phase shift relative to the magneto output. No phase shift occurs during the NS forcing of the shaker because the eccentric force is exciting the building at a non-resonance frequency in the translational NS direction. Figs. 8-10 show the 2^{nd} EW mode that occurs at 4.7 Hz, the 2^{nd} NS mode at 7.2 Hz, and the 2^{nd} torsional mode at 7.7 Hz. The phase shift experiment results are summarized in Table 1. For simplicity, a phase shift of 0^o is assigned for all

the non-resonant situations (i.e. when the two oscillations are either 0^o or 180^o out-of-phase) (Table 1).

3. Deterministic-stochastic subspace identification

We now verify our newly identified natural frequencies of Millikan Library with a commonly used input-output system identification method. This is to provide an independent measure of building properties in order to validate the results using the phase shift method. Deterministic-stochastic subspace identification assumes that the dynamic behavior of a building can be modeled by an n^{th}-degree-of-freedom spring-mass system as

$$M\ddot{U}(t) + C\dot{U}(t) + KU(t) = F(t) \tag{2}$$

where $M\epsilon\mathbb{R}^{nxn}$ is the mass matrix; $C\epsilon\mathbb{R}^{nxn}$ is the damping matrix; $K\epsilon\mathbb{R}^{nxn}$ is the stiffness matrix; $U(t)\epsilon\mathbb{R}^{nx1}$ is the displacement vector; and $F(t)\epsilon\mathbb{R}^{nx1}$ is the excitation force as a function of continuous time *t*.

Eq. 2 describes a model in continuous time, whereas measurements are always obtained as discrete time samples. By applying discretization and including modeling noise, the linear time-invariant structural model can be converted to a discrete-time subspace model as

$$x_{k+1} = Ax_k + Bu_k + w_k \tag{3}$$
$$y_k = Cx_k + v_k \tag{4}$$

where $x_k\epsilon\mathbb{R}^{nx1}$ is the discrete state vector; $y_k\epsilon\mathbb{R}^{Nx1}$ is the sampled output vector; $u_k\epsilon\mathbb{R}^{Nx1}$ is the sampled input vector; $w_k\epsilon\mathbb{R}^{nx1}$ is the process noise vector (mainly due to modeling inaccuracies); $v_k\epsilon\mathbb{R}^{Nx1}$ is the measurement noise vector (mainly due to sensor inaccuracies); $A\epsilon\mathbb{R}^{nxn}$, $B\epsilon\mathbb{R}^{nxn}$, and $C\epsilon\mathbb{R}^{Nxn}$ are the system matrices; *k* is the time sampling instant; *n* is the system order; and *N* is the number of input/output samples. The state noise is assumed to be zero-mean Gaussian white noise. Detailed derivations of the mathematical setup can be found in Overschee and Moor (1994), Ljung (1999), and Guyader and Mevel (2003).

Theoretically, the properties of a system with *n* degrees-of-freedom can be modeled by a subspace model with order *N=2n*. In practice, determination of the most probable model order is not trivial due to noise present in the system, including modeling inaccuracies and measurement noise. A common practice is to use a stabilization plot to distinguish stable modes of the system from spurious modes (Peeters and Roeck, 2001; Altunisik et al., 2011; Döhler et al., 2011). An N^{th} order subspace system contains *N* numbers of modes. Modal parameters of the system for the i^{th} mode can be obtained from Eqs. 5-7. The modes of each system order will be compared to those with a

lower system order. If the frequency, damping ratio, and associated mode shape (usually calculated as modal assurance criterion values) differences are within certain limits, the particular mode is labeled as stable. Modal parameters (frequency f_i, damping ratio ζ_i, and mode shape Φ_i) can be obtained from the eigenvalue λ_i and eigenvector φ_i of system matrix A as

$$f_i = \frac{|ln(\lambda_i)|}{2\pi\,\Delta t} \tag{5}$$

$$\zeta_i = \frac{-2\pi\,Re[|ln(\lambda_i)|]}{f_i\,\Delta t} \tag{6}$$

$$\Phi_i = C\varphi_i \tag{7}$$

Seismic records of Millikan Library during two earthquakes, the M4.4 August 9, 2007 Chatsworth CA earthquake and the M7.2 April 4, 2010 El Mayor Cucapah (Baja California) earthquake, were selected for system identification. The data were recorded by Kinemetrics FBA-11 sensors on a 16-bit real-time datalogger monitoring system (RTMS) of Digitexx Data Systems, Inc. The channels in both the NS and EW directions at each floor were used. The channels at the basement level were used as sample input, while the other channels from the 1st floor to the roof were used as sample output. The data were downsampled from 200 to 100 samples per second incorporating a Chebyshev Type I filter.

Stabilization plots with system order from 5 to 80 for the selected earthquakes are shown in Figs. 11-12. A mode is called stable in this study if the frequency difference between two successive orders is less than 1%, the damping ratio difference is less than 5%, and the mode shape difference is less than 2% using the modal assurance criterion. A mode that remains stable for six successive system orders is considered a physical mode for Millikan Library. The identified modes for the 2007 Chatsworth CA earthquake are 1.16 Hz, 1.75 Hz and 4.76 Hz, 7.03 Hz and 10.0 Hz. The identified modes for the 2010 El Mayor Cucapah earthquake are 1.09 Hz, 1.66 Hz, 4.62 Hz, 6.98 Hz and 10.5 Hz. The associated damping ratio for each mode identified by the subspace method is less than 5%, which is within the expected range for this type of building. Results are summarized in Table 2.

4. Discussion

Table 2 compares the previously proposed (Bradford, 2006) and the newly identified natural frequencies for Millikan Library. Since the frequency sweep experiment was performed at increments of 0.05 Hz, the results from phase shift analysis are limited to the resolution of this frequency increment, but they can be used to confirm or refute the previously reported natural frequencies. The 1st mode frequencies from the phase shift experiment (~1.15 Hz for EW, ~1.7 Hz for NS, and ~2.4 Hz for torsion) and subspace system identification (1.09-1.16 Hz for EW and 1.66-1.75 Hz for NS; 1st torsion was not identified) match well with the previously proposed frequencies. Similarly, the 2nd mode frequencies in translational motion from the phase shift experiment (~4.7 Hz

for EW and ~7.2 Hz for NS) agree with the results from subspace system identification (4.62-4.76 Hz for EW and 6.98-7.04 Hz for NS). The results validate the previously identified natural frequencies for the 1st mode (NS, EW, and torsion) as well as the 2nd NS and EW modes. The phase shift results refute the previously identified 3rd EW mode and 2nd torsional mode, because these do not generate a 90° phase shift. The 2nd torsional mode of ~7.7 Hz identified in this study by the phase shift experiment was previously misinterpreted as the 3rd EW mode. Finally, a 3rd EW mode at 10.0-10.5 Hz is suggested by the subspace system identification.

In this newly defined set of natural frequencies, the mode shapes are shown to be independent of each other (Figs. 13-15). The newly defined EW mode shapes have no zero-crossings for the 1st mode, one zero-crossing for the 2nd mode and two zero-crossings for the 3rd mode. This finding also supports the implication that the previous study misinterpreted the 2nd torsional and 3rd EW modes. Note that this frequency (10.0-10.5 Hz) exceeds the safe operation of the shaker and cannot be verified by the phase shift analysis. There is a minor variation in the identified natural frequencies between the two proposed methods, but this is not uncommon. Previous studies show that the natural frequencies of Millikan Library during forced vibrations are 4% lower than those during ambient vibration (Bradford, 2006; Clinton et al., 2006). Also, lower natural frequencies are detected when a larger shaking force is used in the forced vibrations. In this study, earthquake data are used in the subspace system identification and forced vibration data are used in the phase shift analysis. Clinton et al. (2006) found that a seismic event may cause a drop of up to 30% in natural frequency.

In a separate study (Cheng and Heaton, 2013), a simple Timoshenko beam (combined effect of shearing and bending) with rocking-type soil-structure interaction is used to estimate first-order building response using the frequency ratios. Unlike the translational modes of Millikan Library which appear to cause global bending as well as shearing, the torsional modes of a structure primarily involve shearing along the vertical axis; thus the frequency ratios should theoretically approach that of a shear beam. That is, for a uniform shear beam, if ω_0 is the frequency of the 1st mode, then the frequency of the 2nd mode is $3\omega_0$ and the 3rd mode is $5\omega_0$. The ratio of the first two torsional frequencies (2.4 Hz and 7.7 Hz) of Millikan Library is 3.2 Hz, which is close to the behavior of a uniform shear beam. The third torsional mode is expected at $5\omega_0$, or 12.5 Hz. Solely based on the 1st and 2nd natural frequencies of Millikan Library, the 3rd natural frequency is estimated to be 15.3 Hz for the NS direction and 10.0 Hz for the EW direction using this simple Timoshenko beam approach. The prediction in EW direction agrees with the result from the subspace system identification (Table 2). There are some stable modes identified by the subspace method at around 15 Hz, but they do not appear in a consistent way to be quantified as a physical mode. Frequencies above 10.0 Hz are beyond the safe operation of the shaker, so future investigation is needed for conclusive verification of the 3rd vibrational modes.

5. Conclusions

The natural frequencies of the 9-story reinforced concrete Millikan Library building have been revisited using a simple and robust phase shift analysis. This method can successfully identify higher modes of the building and it complements the traditional subspace system identification which does not use phase shift measurements. To measure the shaker's cyclic motion, a simple magneto device was constructed to record shaker phase data. A magneto coil was affixed to the cage of the shaker and a tiny magnet was attached to the bucket (for holding lead weights) of the shaker. The phase shift between the building's response and the driving force was measured from a voltage jump generated each time the magnet passed under the magneto device when the counter-rotating buckets overlapped.

A new set of natural frequencies for Millikan Library is proposed, and the associated mode shapes are shown to be independent of each other. The new frequencies are 1.15 Hz (1st EW), 1.7 Hz (1st NS), 2.4 Hz (1st torsion), 4.7 Hz (2nd EW), 7.2 Hz (2nd NS) and 7.7 Hz (2nd torsion). The newly identified 2nd torsional mode was misinterpreted in previous studies as the 3rd EW mode. This interpretation is compatible with the results from subspace system identification based on two sets of earthquake records. The subspace method also suggests that the 3rd EW mode may occur in the range of 10.0-10.5 Hz.

Acknowledgements

This work is partially supported by the National Science Foundation (EAR-1027790), George Housner Earthquake Engineering Research Endowment (EAS-41212), Fred L. Hartley Family Foundation, and Croucher Foundation. Their support is gratefully acknowledged.

References

Altunisik, A.C., Bayraktar, A., and Sevim, B. (2011). "Output-only system identification of post-tensioned segmental concrete highway bridges." *Journal of Bridge Engineering* 16(2), 259-266.

Arakawa, T. and Yamamoto, K. (2004). "Frequencies and damping ratios of a high rise building based on microtremor measurement." *Proc., 13th World Conference on Earthquake Engineering*, Vancouver, Canada.

Bradford, S. C., Clinton, J. F., Favela, J., and Heaton, T. H. (2004). "Results of Millikan Library forced vibration testing." *Technical Report Caltech-EERL: EERL-2004-03*, California Institute of Technology, Pasadena, CA.

Bradford, S. C. (2006). "Time-frequency analysis of systems with changing dynamic properties." *PhD Dissertation*, California Institute of Technology, Pasadena, CA.

Cheng, M. H., and Heaton, T. H. (2013). "Simulating building motions using the ratios of its natural frequencies and a Timoshenko beam model." *submitted to Earthquake Spectra*.

Chopra, A. K. (2007). "Dynamics of structures: Theory and applications to earthquake engineering." Third edition. *Prentice Hall*, Upper Saddle River, NJ.

Clinton, J. F., Bradford, S. C., Heaton, T. H., and Favela, J. (2006). "The observed wander of the natural frequencies in a structure." *Bulletin of the Seismological Society of America* 96(1), 237-257.

Döhler, M., Hille, F., Mevel, L., and Rücker, W. (2011). "Structural health monitoring during progress damage test of S101 bridge." *Proc., 8th International Workshop on Structural Health Monitoring*, Stanford, CA.

Foutch, D. A. and Jennings, P. C. (1978). "A study of the apparent change in the foundation response of a nine-story reinforced concrete building." *Bulletin of the Seismology Society of America* 68(1), 219-229.

Guyader, A. and Mevel, L. (2003). "Covariance-driven subspace methods: input/output vs output-only." *Proc., 21st International Modal Analysis Conference (IMAC-XXI)*, Kissimmee, Fl.

Li, Q., Yang, S. K., Zhang, N., Wong, C. K., and Jeary, A. P. (2002). "Field measurements of amplitude-dependent damping in a 79-storey tall building and its effects on the structural dynamic responses." *The Structural Design of Tall Buildings* 11, 129-153.

Ljung, L. (1999). "System Identification: Theory for the User." Second Edition, *Prentice-Hall*, Upper Saddle River, NJ.

Luco, J. E., Trifunac, M. D. and Wong, H. L. (1987). "On the apparent change in dynamic behavior of a nine-story reinforced concrete building." *Bulletin of the Seismology Society of America* 77(6), 1961-1983.

Michel, C. and Gueguen, P. (2010). "Time-frequency analysis of transitory/permanent frequency decrease in civil engineering structures during earthquakes." *Structural Health Monitoring* 9(2), 159-171.

Moaveni, B. and Asgarieh, E. (2012). “Deterministic-stochastic subspace identification method for identification of nonlinear structures as time-varying linear systems.” *Mechanical Systems and Signal Processing* 31, 40-45.

Overschee, P. V. and Moor, B. D. (1994). “N4SID: subspace algorithms for the identification of combined deterministic-stochastic systems.” *Automatica* 30(1), 75-93.

Peeters, B. and Roeck, G. D. (2001). “Stochastic system identification for operational modal analysis: a review.” *Journal of Dynamic Systems, Measurement, and Control* 123, 659-667.

Piekarski, B., DeVoe, D., Dubey, M., Kaul, R., and Conrad, J. (2001). “Surface micromachined piezoelectric resonant beam filters.” *Sensors and Actuators* 91, 313-320.

Scheible, D. V. and Blick, R. H. (2004). “Silicon nanopillars for mechanical single-electron transport.” *Applied Physics Letters* 84(23), 4632-4634.

Taylor, J. R. (2005). “Classical mechanics.” *Unveristy Science Books*, Sausalito, CA.

Todorovska, M. I. (2009a). “Seismic interometry of a soil-structure interaction model with coupled horizontal and rocking response.” *Bulletin of the Seismological Society of America* 99(2A), 611-625.

Todorovska, M. I. (2009b). “Soil-structure system identification of Millikan Library North-South response during four earthquakes (1970-2002): what caused the observed wandering of the system frequencies?” *Bulletin of the Seismological Society of America* 99(2A), 626-635.

Udwadia, F. E. and Trifunac, M. D. (1974). “Time and amplitude dependent response of structures.” *Journal of Earthquake Engineering and Structural Dynamics* 2, 359-378.

Wang, H., Li, J., and Zhang, K. (2008). “Non-resonant response, bifurcation and oscillation suppression of a non-autonomous system with delayed position feedback control.” *Nonlinear Dyn* 51, 447-464.

Zhou, D. F., Hansen, C. H., and Li, J. (2011). “Suppression of maglev vehicle-girder self-excited vibration using a virtual tuned mass damper.” *Journal of Sound Vibration* 330, 883-901.

Tables

Table 1. Phase shift experiment results.

Driving frequency	EW-shaking		NS-shaking	
	EW response	NS response	EW response	NS response
1.15 Hz	90^o	90^o	0^o	0^o
1.7 Hz	0^o	90^o	0^o	90^o
2.4 Hz	90^o	90^o	0^o	0^o
4.7 Hz	90^o	0^o	0^o	0^o
7.2 Hz	0^o	0^o	0^o	90^o
7.7 Hz	90^o	90^o	0^o	0^o

Note: Since some parts of the building are oscillating in phase when the driving force is at higher non-resonant frequencies, while other parts are out of phase, the phase shift values are set to 0^o for all non-resonant situations.

Table 2. Newly identified natural frequencies for Millikan Library.

	Previously Proposed (Bradford, 2006)	Subspace System Identification (this study)		Phase Shift (this study)
		Chatsworth EQ	Baja California EQ	
1st EW	1.14 Hz [1.19 Hz] (2.3%)	1.16 Hz (2.3%)	1.09 Hz (3.6%)	~1.15 Hz
1st NS	1.67 Hz [1.72 Hz] (2.4%)	possibly 1.75 Hz (2.8%)	1.66 Hz (1.9%)	~1.7 Hz
1st Tor	2.38 Hz [2.46 Hz] (1.4%)	-	-	~2.4 Hz
2nd EW	4.93 Hz	4.76 Hz (1.8%)	4.62 Hz (2.5%)	~4.7 Hz
2nd NS	7.22 Hz	7.04 Hz (2.4%)	6.98 Hz (3.7%)	~7.2 Hz
2nd Tor	6.57 Hz	-	-	~7.7 Hz
3rd EW	7.83 Hz	10.0 Hz (1.9%)	10.5 Hz (2.7%)	-

Note: Previously proposed natural frequencies were obtained from forced vibrations, except those in [·] which were obtained from free vibrations. Percentage values in (·) are the associated damping ratios.

Figures

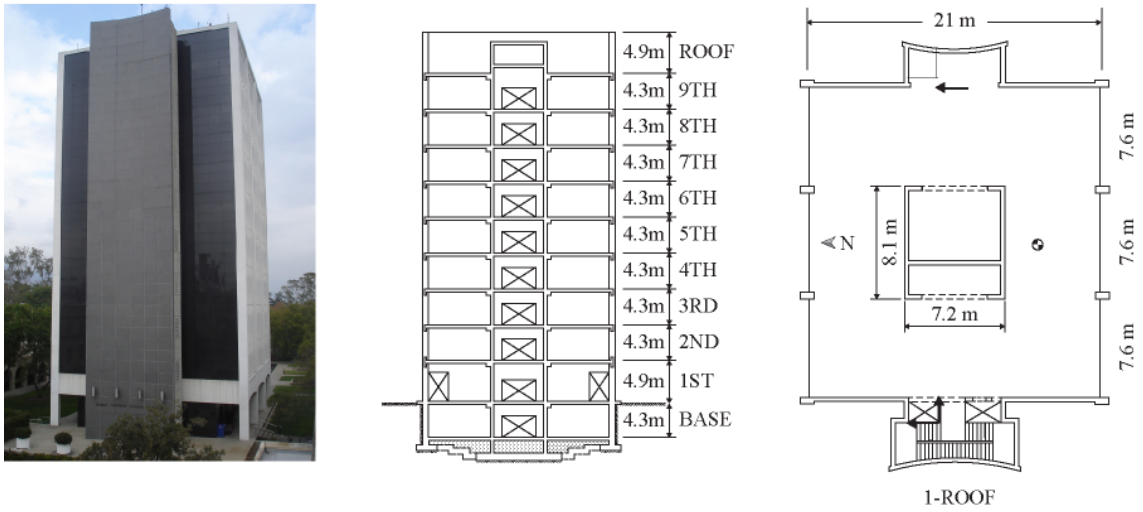

Figure 1. Millikan Library building on the Caltech campus showing building dimensions, floor heights and seismic network configuration (from Bradford, 2006).

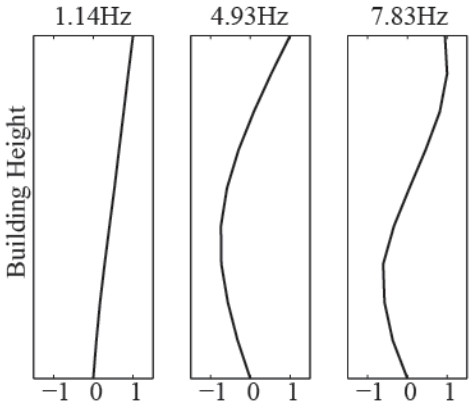

Figure 2. Mode shapes proposed by Bradford (2006) for the 1st (1.14 Hz), 2nd (4.93 Hz) and 3rd (7.83 Hz) EW modes. This 3rd EW mode is problematic because the corresponding mode shape is not independent of the other EW mode shapes.

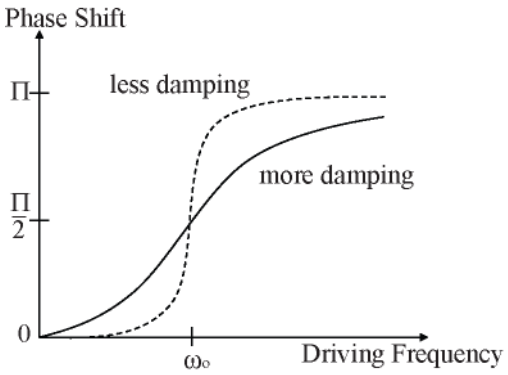

Figure 3. Phase shift versus forced vibration driving frequency schematic.

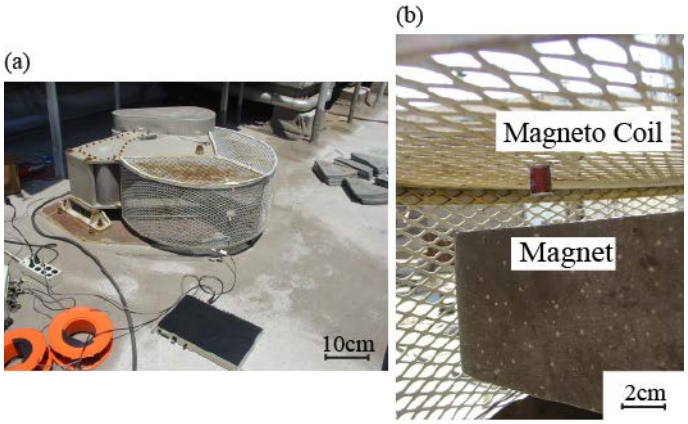

Figure 4. Magneto device installed on the shaker installed on the roof of Millikan Library. (a) Roof shaker. (b) Side view of magneto device.

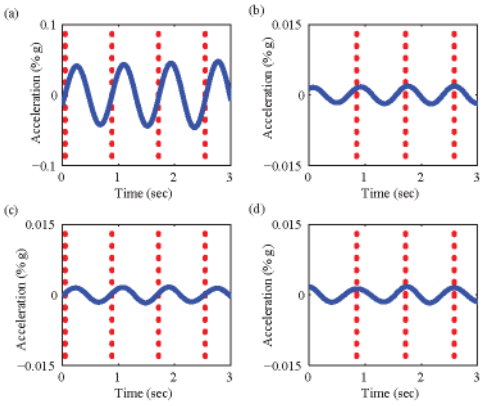

Figure 5. Magneto output of the shaker (dotted line) and building roof acceleration time history (solid line) at 1.15 Hz, which is the 1st EW mode. The magneto produces a current when the sinusoidal shaker force is at a maximum. (a) EW response during EW shaking. (b) EW response during NS shaking. (c) NS response during EW shaking. (d) NS response during NS shaking.

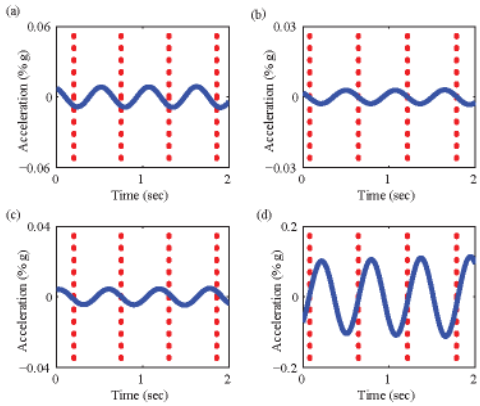

Figure 6. Magneto output of the shaker (dotted line) and building roof acceleration time history (solid line) at 1.7 Hz, which is the 1st NS mode. (a) EW response during EW shaking. (b) EW response during NS shaking. (c) NS response during EW shaking. (d) NS response during NS shaking.

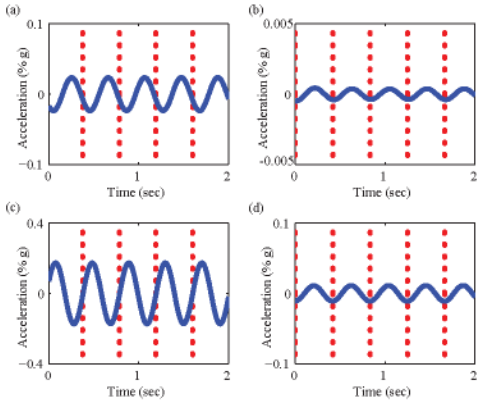

Figure 7. Magneto output of the shaker (dotted line) and building roof acceleration time history (solid line) at 2.4 Hz, which is the first torsional mode. The shaker is near the NS centerline of the building, but it is significantly offset to the south of the EW centerline, so only EW shaking excites the torsional modes. (a) EW response during EW shaking. (b) EW response during NS shaking. (c) NS response during EW shaking. (d) NS response during NS shaking.

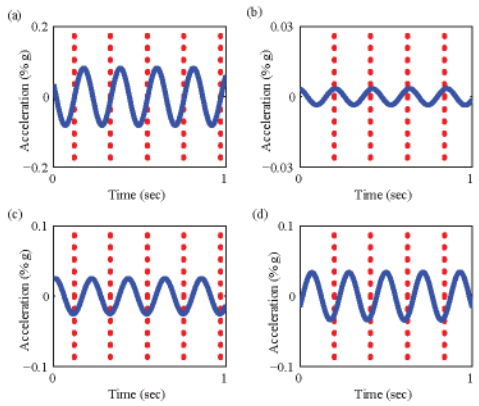

Figure 8. Magneto output of the shaker (dotted line) and building roof acceleration time history (solid line) at 4.7 Hz, which we interpret as the 2nd EW mode. (a) EW response during EW shaking. (b) EW response during NS shaking. (c) NS response during EW shaking. (d) NS response during NS shaking.

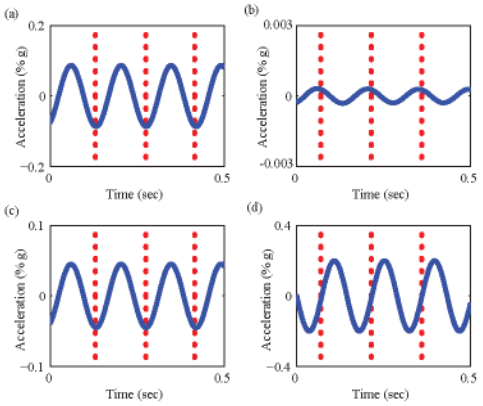

Figure 9. Magneto output of the shaker (dotted line) and building roof acceleration time history (solid line) at 7.2 Hz, which we interpret as the 2nd NS mode. (a) EW response during EW shaking. (b) EW response during NS shaking. (c) NS response during EW shaking. (d) NS response during NS shaking.

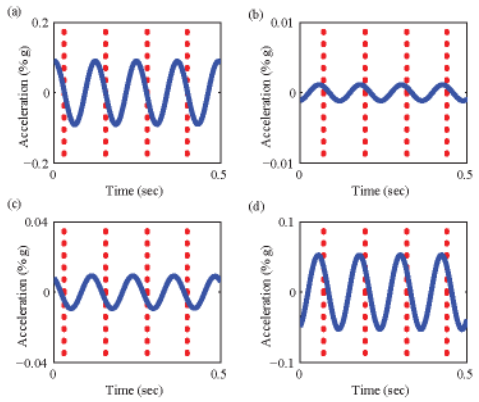

Figure 10. Magneto output of the shaker (dotted line) and building roof acceleration time history (solid line) at 7.7 Hz, which we newly interpret as the 2nd torsional mode. (a) EW response during EW shaking. (b) EW response during NS shaking. (c) NS response during EW shaking. (d) NS response during NS shaking.

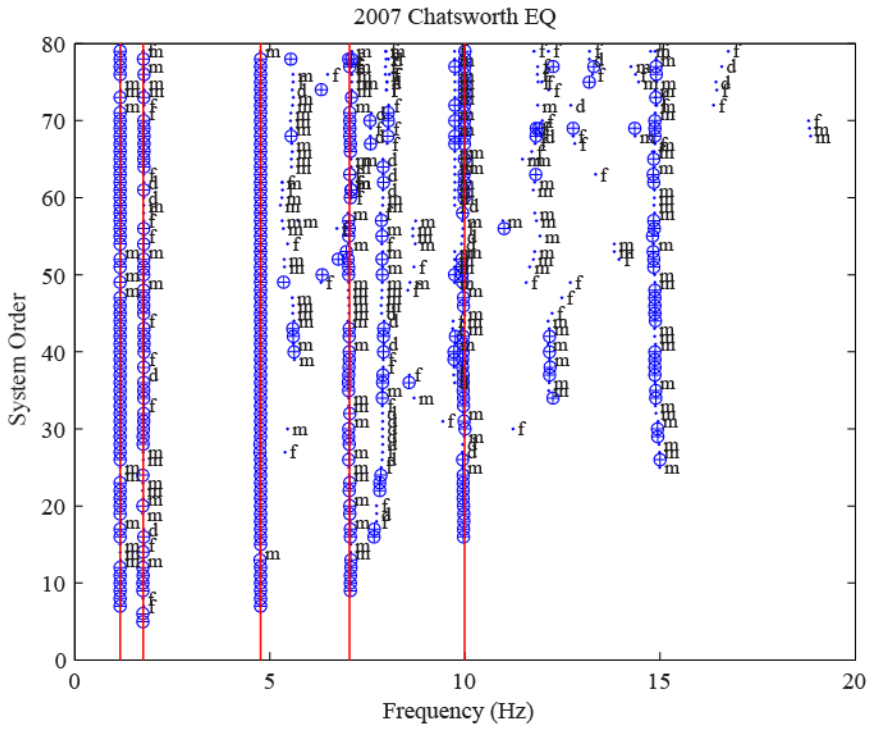

Figure 11. Stabilization plot for the 2007 Chatsworth, CA earthquake. The symbols are: "⊕" for a stable mode; ".d" for a mode with stable frequency and damping; ".m" for a mode with stable frequency and mode shape; and ".f" for a mode with stable frequency. The solid lines represent identified physical modes for Millikan Library.

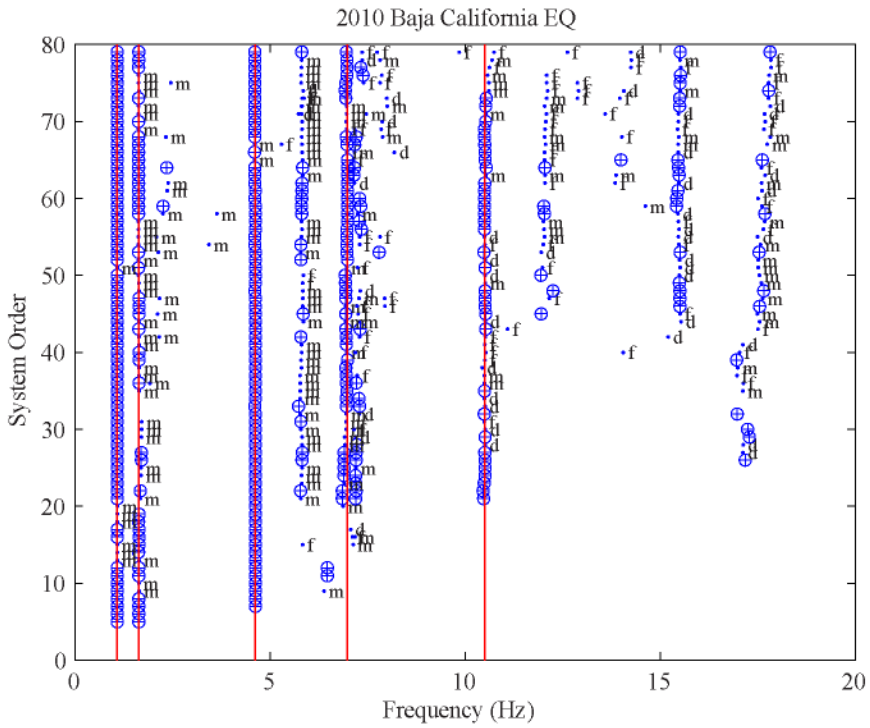

Figure 12. Stabilization plot for the 2010 El Mayor Cucapah earthquake. The symbols are: "⊕" for a stable mode; ".d" for a mode with stable frequency and damping; ".m" for a mode with stable frequency and mode shape; and ".f" for a mode with stable frequency. The solid lines represent identified physical modes for Millikan Library.

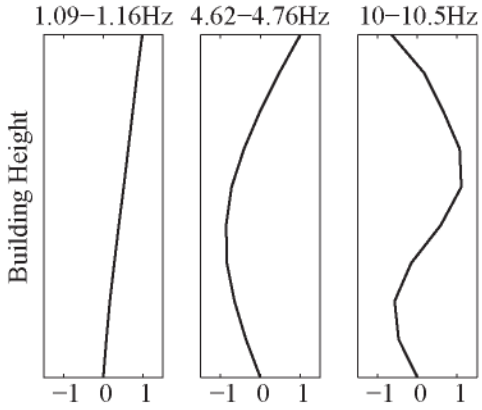

Figure 13. Mode shapes for the 1st (1.09-1.16 Hz), 2nd (4.62-4.76 Hz) EW modes, and 3rd (10.0-10.5 Hz) EW mode identified by subspace system identification.

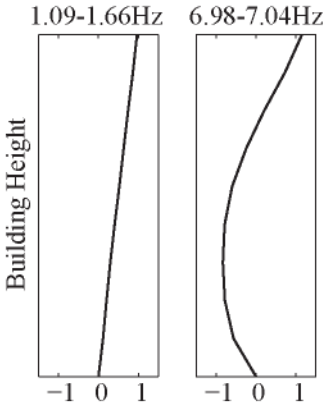

Figure 14. Mode shapes for the 1st (1.66-1.75 Hz) and 2nd (6.98-7.04 Hz) NS mode identified by subspace system identification.

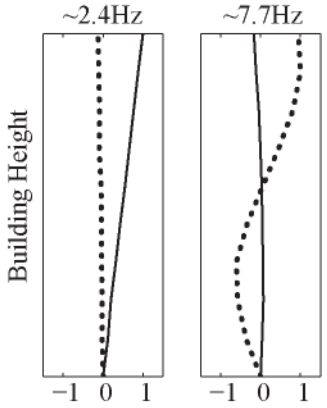

Figure 15. Mode shapes from Bradford (2006) which were defined as the 1st torsional mode and the 3rd EW mode. We, however, find that these are actually associated with the 1st torsional mode with a frequency of 2.4 Hz, and the 2nd torsional mode with a frequency of 7.7 Hz. Solid line shows the normalized amplitude for the NS component, and the dotted line shows the EW component.